Volume: 6 Issue: 2 Pages: 2222-2232 (2014) ISSN : 0975-0290

Applying Content-Based Image Retrieval Techniques to Provide New Services for Tourism Industry

Zobeir Raisi
Department of Electrical Engineering, Chabahar Maritime University, Chabahar, IRAN
Email: zobeir.raisi@cmu.ac.ir
Farahnaz Mohanna
Assistant professor, Faculty of Electrical and Computer Engineering, University of Sistan and Baluchestan, Zahedan, IRAN
Email: f_mohanna@ece.usb.ac.ir
Mehdi Rezaei
Assistant professor, Faculty of Electrical and Computer Engineering, University of Sistan and Baluchestan, Zahedan, IRAN
Email: mehdi.rezaei@ece.usb.ac.ir

----------**ABSTRACT**----------
The aim of this paper is to use the network and internet and also to apply the content based image retrieval techniques to provide new services for tourism industry. The assumption is a tourist faces an interesting subject; he or she can take an image of subject by a handheld device and send it to the server as query image of CBIR. In the server, images similar to the query are retrieved and results are returned to the handheld device to be shown on a web browser. Then, the tourist can access the useful information about the subject by clicking on one of the retrieved images. For this purpose, a tourism database is created. Then several particular content-based image retrieval techniques are selected and applied to the database. Among these techniques, 'Edge Histogram Descriptor (EHD)' and 'Color layout descriptor (CLD)' algorithms have better retrieval performances than the others. By combining and modification of these two methods, a new CBIR algorithm is proposed for this application. Simulation results show a high retrieval performance for the proposed algorithm.

Keywords – CBIR, Tourism Industry, MPEG-7, Mobile, Handheld Device
---
Date of Submission : August 06, 2014 Date of Acceptance : September 29,2014

1. INTRODUCTION

Nowadays, with the explosive growth of the number of digital images available on internet and the availability of image capturing devices such as digital cameras and image scanners, the size of digital products is increasing rapidly [1, 2], therefore efficient indexing and searching becomes essential for large image archives. For this purpose, many general-purpose image retrieval systems have been developed. There are three categories of image retrieval methods: text-based, content-based, and semantic based. In text-based systems, the images are manually annotated by text descriptors. Text annotation to all images manually is impractical because of large labeling cost and the subjective of human perception. To overcome the above disadvantages in text-based image retrieval system, 'Content-Based Image Retrieval (CBIR)' was introduced in the early 1980s, which is based on automatically indexing and retrieval [3, 4]. CBIR aims to search images that are perceptually similar to the query image based on visual content of the images without the help of annotations. Researches mainly focused on the effective low-level representation of images and CBIR usually indexes images by low-level visual features such as color [5], texture [6], and shape [7].

Color is the most dominant and distinguishing visual feature that is widely used in CBIR and is invariant to image size and orientations [8, 9]. As conventional color features used in CBIR, there are color histogram, color correlogram, color structure descriptor, and scale color descriptor [2]. Color histogram is the most commonly used color representation scheme to represent the global feature composition of an image but it does not have any spatial information. It is invariant to translation and rotation of an image and normalizing the histogram lead to scale invariance [10].

Texture is used to specify the roughness or coarseness of object surface and described as a pattern with some kind of regularity. Texture feature has been used in various applications ranging from industrial application to medical imaging. There are various algorithms for texture analysis used by researches, such as gray co-occurrences matrix [11], Markov random field [12], 'simultaneous auto-regressive (SAR)' model [13], wold decomposition model [14], Gabor filtering [15], wavelet decomposition [16] and so on[7, 8].

Shape features are important image features though they have not been widely used in CBIR as color and texture features. Accurate extraction and representation of shape information is one of the challenging tasks in shape image retrieval [17]. Shape features have shown to be useful in many domain specific images such as man-made objects. For color images used in most papers, however, it is difficult to apply shape features compared to color and texture due to the inaccuracy of segmentation [7]. The classic methods of

Volume: 6 Issue: 2 Pages: 2222-2232 (2014) ISSN : 0975-0290

describing shape features are moment invariants, Fourier transform coefficients, edge curvatures, and arc length [7].

The mobile phone industry is going to change phenomenally over the past few years with significant advances in areas of communications and multimedia. Currently, the state-of-the-art multimedia compliant handheld devices such as mobile phones, equipped with digital camera and wireless network connection, enable accessing to large amount of digital media [18]. Moreover, such a powerful device enables new applications. In [19], a client-server content-based image retrieval framework for mobile platforms is developed, which provides the capability of content-based query and browsing from mobile devices. The proposed framework provides an adaptive user interface and a generic structure, which supports a wide range of mobile devices.

Regarding the proposed framework in [19], as a new application, we propose a scenario in which handheld devices and CBIR are used for tourism application. In the proposed scenario a CBIR algorithm is run by a server on a database of images taken from places or other subjects that may be interesting for tourists. Several images of each place or subject exist in the database while useful information is provided about the subject on the server. When a tourist faces an interesting subject, he or she can take an image of subject by a handheld device and send it to the server as a query image of CBIR system. In the server, images similar to the query are retrieved and results are returned to the handheld device to be shown on a web browser. Then, the tourist can access the useful information about the subject by clicking on one of the corrected retrieved images. Fig. 1 shows the scheme of the proposed system.

In this research, a study was carried out on several CBIR methods, currently proposed by researchers. The methods employed color, texture, and edge features to characterize a query image. The methods were then compared based on their accuracy, running time, and suitability for our application. In this regard, a database was prepared including 1000 images taken from attractions of Zahedan city and University of Sistan and Baluchestan. The photographs were taken in different times of a day and from different view angles and distances. In addition, all the CBIR methods, tested on our data base, were applied to Corel_1k database [20] and the performance of the methods on two databases were compared to each other. Finally, a new CBIR algorithm is proposed that performs well for our application.

The rest of the paper is organized as follow. Section II introduces a brief overview and comprehensive survey on several recently published image retrieval methods. Section III describes the proposed methods. Section IV presents experimental results of applying these CBIR methods to our database and Corel_1k database. The paper is concluded in Section V.

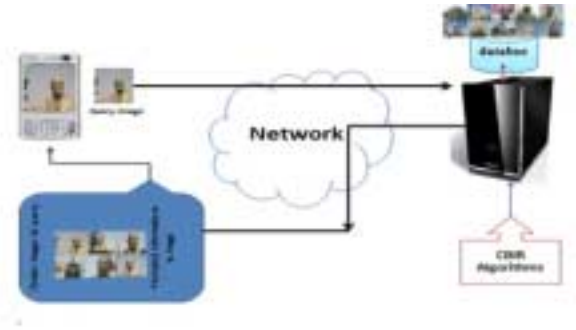

Fig. 1: Proposed System

2. STUDIED CBIR METHODS

2.1. CLD

The MPEG-7 'Color Layout Descriptor (CLD)' is designed to represent the spatial distribution of the color features in an image [21]. It is based on generating a tiny (8x8) thumbnail of an image, which is encoded via 'Discrete Cosine Transform (DCT)' and quantized. During the CLD extraction process, it is assumed that the image consists of three color channels, R, G and B. The steps of CLD descriptor is demonstrated in Fig. 2 and Fig. 3.

The feature extraction process consists of two steps: first the input image is divided into 8x8 non-overlapping blocks and a representative color for each block is determined. Then, the representative color of 8x8 blocks are transformed into YCbCr color space to obtain a down-sampled version of the image. Average color of each block is computed and used as representative color for each block. The CLD is obtained by applying 2-D DCT on the down sampled image. In the next step, a set of low frequency DCT components of each YCbCr plane are selected in zigzag scanning order and quantized to form a CLD [22].

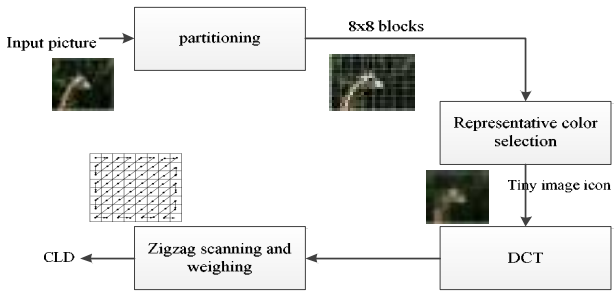

Fig. 2: The CLD extraction process block diagram

Fig. 3: Zigzag scanning in the CLD extraction process

Volume: 6 Issue: 2 Pages: 2222-2232 (2014) ISSN : 0975-0290

In this case, the CLD descriptor was formed by reading in zigzag order first six coefficients from the Y-DCT matrix and three first coefficients from each DCT matrix of the two chrominance components. The descriptor is saved as an array of 12 values (Fig. 3). For matching two CLDs, { DY, DCr, DCb }, and { DY', DCr', DCb' }, the following distance measure is used [22]:

$$D = \sqrt{\sum_i w_{yi}(DY_i - DY_i')^2} + \sqrt{\sum_i w_{bi}(DCb_i - DCb_i')^2} + \sqrt{\sum_i w_{ri}(DCr_i - DCr_i')^2} \quad (1)$$

where (w_{yi}, w_{bi}, w_{ri}), represent the i[th] DCT coefficients of the representative color components. The distances are weighted appropriately, with larger weights given to lower frequency components.

2.2. Edge Histogram Descriptor

The EHD method is an efficient texture descriptor for images with textual purchase and it can also work as a shape descriptor as long as the edge field contains the true object boundaries. The MPEG-7 'Edge Histogram Descriptor (EHD)' represents the distribution of 5 edge types in each local area called sub-image which are: vertical, horizontal, 45-degree diagonal, 135- degree diagonal, and non-edge (Fig. 4)[21, 22]. An example image is shown in Fig. 5. In this example the sub-images are defined by dividing the image into 16 non-overlapping blocks. To characterize the EHD, each sub-image serves a basic region to generate an edge histogram which consists of 5 bins corresponding to vertical, horizontal, 45-degree diagonal, 135- degree diagonal, and non-directional edge types. Thus, the histogram for each sub-image represents the relative frequency of occurrence of edge types in the corresponding sub-image. For example, an image with 16 sub- images yields a local edge histogram with a total of 80 bins. These 80 histogram bins are the only standardized semantics for the MPEG-7 edge histogram descriptor. By scanning sub-images according to the order shown in Fig. 3, the semantics of the bins are defined as in **Error! Reference source not found.**1. These 80 normalized and quantized bins constitute the standardized EHD of MPEG-7.

Histogram bins	Semantics
Local_Edge [0]	Vertical edge of sub-image at (0,0)
Local_Edge [1]	Horizontal edge of sub-image at (0,0)
Local_Edge [2]	45 degree edge of sub-image at (0,0)
Local_Edge [3]	135 degree edge of sub-image at (0,0)
Local_Edge [4]	Non-directional edge of sub-image at (0,0)
Local_Edge [5]	Vertical edge of sub-image at (0,1)
. . . .	. . . .
Local_Edge [74]	Non-directional edge of sub-image at (3,2)
Local_Edge [75]	Vertical edge of sub-image at (3,3)
Local_Edge [76]	Horizontal edge of sub-image at (3,3)
Local_Edge [77]	45degree edge of sub-image at (3,3)
Local_Edge [78]	135 degree edge of sub-image at (3,3)
Local_Edge [79]	Non-directional edge of sub-image at (3,3)

Table 1: Semantics of local edge bins

To extract edge features, each sub-image or image-block is further divided into four sub-blocks (Fig. 6). Then, the luminance values of the four sub-blocks are used for the edge detection. The luminance mean values of four sub-blocks are convolved with coefficients of five edge detection filters shown in Fig. 7 to obtain the edge magnitudes. More specifically, the sub-blocks are labelled from 0 to 3 as shown in Fig. 6. For the k[th] (k=0, 1, 2, 3) sub-block of the (i, j)[th] image-block, the average grey level $a_k(i, j)$ is calculated. The filter coefficients for vertical, horizontal, 45-degree diagonal, 135-degree diagonal, and

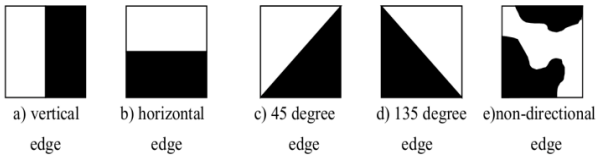

Fig. 4: Five types of edges

Fig. 5: Definition of sub-image and image-blocks

Non-directional edges are denoted as $f_v(k)$, $f_h(k)$, $f_{d-45}(k)$, $f_{d-135}(k)$ and $f_{nd}(k)$ respectively. Now the respective edge magnitudes $m_v(i, j)$, $m_h(i, j)$, $m_{d-45}(i, j)$, $m_{d-135}(i, j)$ and $m_{nd}(i, j)$ for the (i, j) [th] image-block can be obtained as follows [23, 24]:

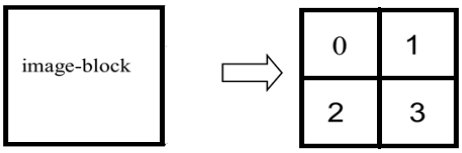

Volume: 6 Issue: 2 Pages: 2222-2232 (2014) ISSN : 0975-0290

Fig. 6: Sub-blocks and their labelling

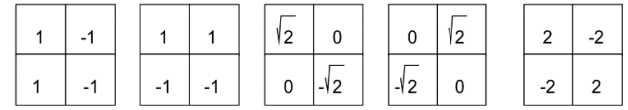

Fig. 7: Filters for edge detection

$$m_v(i,j)=\left|\sum_{k=0}^{3} a_k(i,j)\times f_v(k)\right| \quad (2)$$

$$m_h(i,j)=\left|\sum_{k=0}^{3} a_k(i,j)\times f_h(k)\right| \quad (3)$$

$$m_{d-45}(i,j)=\left|\sum_{k=0}^{3} a_k(i,j)\times f_{d-45}(k)\right| \quad (4)$$

$$m_{d-135}(i,j)=\left|\sum_{k=0}^{3} a_k(i,j)\times f_{d-135}(k)\right| \quad (5)$$

$$m_{nd}(i,j)=\left|\sum_{k=0}^{3} a_k(i,j)\times f_{nd}(k)\right| \quad (6)$$

$$\max\{m_v(i,j), m_h(i,j), m_{d-45}(i,j), m_{d-135}(i,j), m_{nd}(i,j)\} > Th_{edge} \quad (7)$$

If the maximum value among 5 edges magnitude obtained from (2) to (6) is greater than a threshold (Th_{edge}), then the image-block is considered to have the corresponding edge (7). Otherwise, the image-block has no edge. In this paper, the Th_{edge}, was set at 11 according to the experiments.

2.3. Co-occurrence Matrix

Co-occurrence matrix is a texture analysis technique for CBIR [11, 22]. The co-occurrence matrix extracts texture information relevant to higher frequency components accurately. Co-occurrence matrices of a binary image I for a certain Δx and Δy are obtained by the following equation:

$$C_{\Delta x,\Delta y}(i,j)=\sum_{p=1}^{n}\sum_{q=1}^{m}\begin{cases}1, & \text{if } I(p,q)=i \text{ and } I(p+\Delta x, q+\Delta y)=j\\ 0, & \text{otherwise}\end{cases} \quad (8)$$

Here, the offset ($\Delta x, \Delta y$), is specifying the distance between the pixel-of-interest and its neighbor Co-occurrence matrices are computed on the binary image resulted from applying canny edge detector on the gray scale images. Using 12 pairs of ($\Delta x, \Delta y$), including (0, d), (-d, d), (d, 0) and (-d,-d) where d=1, 2, 3, will result 12 matrices with the size of 2x2 and totally 48 real numbers [25].

2.4. Scale Color Descriptor

'Scale Color Descriptor (SCD)' is the one part of MPEG-7 visual standard consisting of color space, color quantization and histogram descriptors [22]. This would allow specification of color histogram with varying number of bins and non-uniform quantization of different color spaces. The SCD uses the HSV color space that is uniformly quantized into a total of 256 bins. This includes 16 levels in H, 4 levels in S and 4 levels in V color model component. The histogram values are truncated into an 11-bit integer representation. Histograms of images with different sizes have different sizes as well. Therefore, different sized histograms can be compared using size conversion provided by Haar transform.

2.5. Dominant Color Descriptor

'Dominant Color Descriptor (DCD)' provides an effective, compact and intuitive representation of colors existing in an image [26]. In this descriptor, image features are formed by a small number of representative colors. These colors are normally obtained by using clustering and color quantization. The DCD in MPEG-7 is defined as:

$$F=\{(c_i,p_i,v_i),s\} \quad (i=1,2,...N), \quad (9)$$

where N is the total number of dominant colors in an image while a region in an image can be presented by a maximum of eight dominant colors. c_i represents a 3-D dominant colors vector, and p_i is the percentage of each dominant color. v_i and s, which are optional, denote the representative color variance and the spatial coherency, respectively.

To extract DCD features of an image different algorithms such as GLA (Generalized Lloyd Algorithm) and FRCFE (Fixed Representative Colors Feature Extraction algorithm) have been used [27]. The GLA is the most extensively used algorithm while it has an expensive computation cost and long running time [27]. For the proposed system in this paper, we used FRCFE that provides a better performance with less computational complexity in comparison with the GLA. In FRCFE, 38 perceptual colors are used to represent an image based on DCDs in RGB space [28]. **Error! Reference source not found.**2 shows these colors selected from the RGB color space.

The steps of FRCFE algorithm are as follow:

- Read the input image and separate R, G, B components of the image for each pixel.
- For each pixel
  - Search color table for nearest color by finding the distance between the pixel color I represented as (P_r, P_g, P_b) and the colors in Table 2 which are presented by c_i as (C_{iR}, C_{iG}, C_{iB}) using equation(10):

S/No	Red	Green	Blue	S/No	Red	Green	Blue
1	255	0	0	20	0	204	255
2	255	102	0	21	200	200	200
3	255	255	153	22	210	210	175
4	255	255	0	23	255	0	255

Volume: 6 Issue: 2 Pages: 2222-2232 (2014) ISSN : 0975-0290

5	128	0	0	24	255	153	204
6	255	153	0	25	0	255	255
7	255	153	51	26	153	51	0
8	0	51	0	27	153	102	51
9	51	153	51	28	102	128	51
10	51	51	0	29	204	102	0
11	128	128	51	30	0	0	0
12	51	153	102	31	255	255	255
13	153	204	0	32	51	102	153
14	0	255	0	33	0	51	102
15	0	128	0	34	0	128	128
16	51	102	255	35	51	51	153
17	153	204	255	36	153	51	102
18	0	0	255	37	204	153	255
19	0	0	128	38	85	75	60

Table 2: Perceptual Dominant Colors Used by DCD

$$C_d = \min\left(\sqrt{(P_r - C_{iR})^2 + (P_g - C_{iG})^2 + (P_b - C_{iB})^2}\right) \quad (10)$$

- Assign to the pixel an entry from RGB color table with minimum c_d .

- Create frequency table for assigned colors.
- Sort the frequency table in descending order.

The highest eight frequent colors and their percentages are then selected to create the description of the image. Sample result of the DCD color quantization using FRCFE for an image is illustrated in Fig. 8

Fig. 8: DCD color quantization using FRCFE

The dissimilarity $D(F1,F2)$ between the two descriptors of DCD can be computed as:

$$D^2(F1,F2) = \sum_{i=1}^{N_1} P_{1_i}^2 + \sum_{j=1}^{N_2} P_{2j}^2 - \sum_{i=1}^{N_1}\sum_{j=1}^{N_2} 2a_{1i,2j}P_{1i}P_{2j} \quad (11)$$

where $a_{1i,2j}$ is the similarity coefficient between two colors c_{1i} and c_{2j} that is defined in (11). It should be noted that $c_{1i} \neq c_{2j}$ since they are from different sets of colors in two descriptors,

$$a_{1i,2j} = \begin{cases} 1 - \left\|c_{1i} - c_{2j}\right\| / \alpha T_d, & \left\|c_{1i} - c_{2j}\right\| \leq T_d \\ 0, & \left\|c_{1i} - c_{2j}\right\| > T_d \end{cases} \quad (12)$$

where $\left\|c_{1i} - c_{2j}\right\|$ is the Euclidean distance between two colors c_{1i} and c_{2j} in CIELuv color space, T_d is the maximum distance for two colors to be considered as similar. A typical value for T_d is between 10 and 20 in the CIELuv color space and for α is between 1.0 and 1.5. The above dissimilarity measure is very similar to the quadratic distance measure that is commonly used in comparing two color histogram descriptors [29, 30]. In this paper, implementation of DCD algorithm carried out by T_d =15 and α =1.16.

2.6. Statistical Color Features

As already mentioned color is an important low level visual feature in CBIR. However, some of the color features such as histogram do not consider spatial distribution. Some other color features are sensitive to scaling and illumination changes, e.g. color correlogram [2, 25]. As new features, the statistics of color in different color space such as RGB and L*a*b* spaces are used to provide complementary information for CBIR. The L*a*b* is a uniform perceptual color space [31]. Especially, its L component closely matches human perception and it is useful in closing the semantic gap in CBIR. Moreover, several works have used RGB color space as well [8, 32, 33]. Here as color features, the statistical values of the two mentioned color spaces are extracted. These values include the first, the second and the third moments. Mean is the first statistical moment. Although the mean of a colored image holds some information about its color features, but it is not enough. In this regard, the standard deviation and skewness used as well, according to the following equations[25]:

$$mean = \frac{1}{MN}\sum_{i=1}^{M}\sum_{j=1}^{N} I(i,j) \quad (13)$$

$$std = \sqrt{\frac{1}{MN}\sum_{i=1}^{M}\sum_{j=1}^{N} (I(i,j) - mean)^2} \quad (14)$$

$$skewness = \sqrt[3]{\frac{1}{MN}\sum_{i=1}^{M}\sum_{j=1}^{N} \left(\frac{I(i,j) - mean}{std}\right)^3} \quad (15)$$

Where, M and N denotes the image dimensions, and I refers to one of the image color components. Therefore, in this research, using three statistical parameters and two color spaces, including L*a*b* and RGB, a feature vector with totally 18 features were generated and used.

3. PROPOSED METHODS

In this paper new CBIR algorithms for the tourism application are proposed. The CBIR methods studied above were implemented and applied to the tourism image data base, provided in this research. According to the studied results, some methods were selected and modified to improve the image retrieval performance in this application. More details about the proposed methods are presented in the sequel.

3.1. Modified EHD with Global and Semi-global Edge Histograms

The EHD method, explained in section B, computes an edge histogram on each sub-image. Then, combining the sub-image histograms in parallel, a new histogram with more

Volume: 6 Issue: 2 Pages: 2222-2232 (2014) ISSN : 0975-0290

number of bins is made over the whole sub-images is called local histogram here. To achieve a higher retrieval performance in the EHD method, beside of the local histogram, we proposed a global and several semi-global histograms which are computed directly from the local histograms. The global histogram is made by adding the sub-image histograms. Therefore, similar to the sub-image histograms, the global histogram includes 5 bins corresponding to 5 edge types. For the semi-global edge histograms, clusters, each including four connected sub-images, are made as shown in Fig. 9.

As illustrated in Fig. 9, there are 13 different clusters; 4 verticals (Fig. 9b), 4 horizontals (Fig. 9c) and 5 overlapping clusters including corners and central sub-images (Fig. 9d) as following:

The first group that is labeled with the number 9, including sub-image numbers: 1, 2, 5 and 6; the second group with number 10 including sub-image numbers: 3, 4, 7 and 8; the third group with number 11 including: 9, 10, 13 and 14; the forth group with number 12 including: 11, 12, 15 and 16 and the fifth group with number 13 including: 6, 7, 10 and 11. Vertical and horizontal clusters are obtained by counting the number of 5 edge type of all sub-images exists in every column and row of an image, respectively. The numbering label is shown in Fig. 9a.

Finally, as each cluster has 5 edge types, we also generate edge distributions for every type. Consequently, our edge histogram has 150 bins including 80 local bins + 5 global bins + 65 semi-global bins (13x5). The overall histogram semantics are demonstrated in Fig. 10.

Therefore in proposed method for each image, the semi-global, global and local histogram is computed. This computation exploited the absolute location of image edges as well as their global composition. As a result, this histogram, which includes 150 bins, will consider as an image feature vector. Therefore, in preprocessing stage of the proposed method, first, for all of the images in the tourism database, semi-global, global and local histogram is computed and store in the database as their feature vectors. Next for retrieval, the comparison of two feature vectors are considered applying (16) which is as follow for two images A, and B.

$$D(A,B) = \sum_{i=1}^{80} \left| Local_A[i] - Local_B[i] \right| + \sum_{i=1}^{5} \left| global_A[i] - global_B[i] \right| + \sum_{i=1}^{65} \left| semiglobal_A[i] - semiglobal_B[i] \right| \quad (16)$$

Equation (16) illustrates the Euclidean distance of two images A and B considering differences of one by one bin of the Local, global and semi-global histogram bins of A and B sub-images.

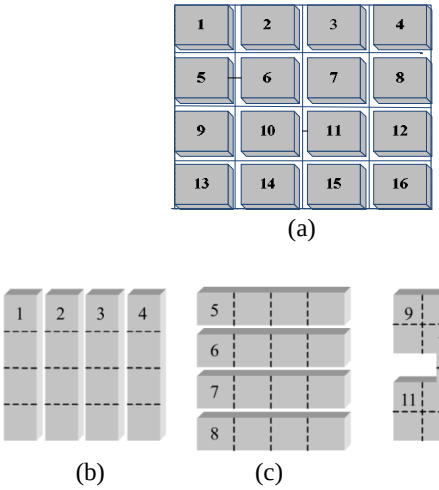

Fig. 9: Clusters of sub-images for semi-global histograms

(a) Sub-image numbering
(b) Horizontal cluster
(c) Vertical cluster
(d) 5 group clusters

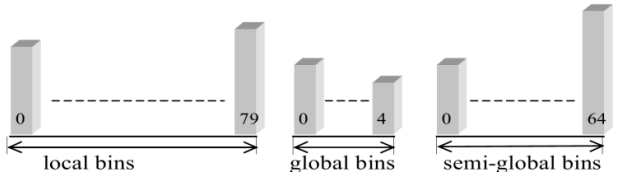

Fig. 10: Overall histogram semantics

3.2. Combination of EHD and CLD

Among the studied image retrieval methods, the EHD and CLD methods are selected and combined together to improve the retrieval performance. These methods are selected because of following reasons. First, EHD and CLD have similar trends in feature extraction such that the features can be localized in terms of sub-images. Moreover, they perform more accurate in image retrieval. Furthermore, image features such as color and edge distribution on each sub-image can be specified independently and combined easily to make a new feature vector. The new feature vector is used by applying a weighted distance as:

$$D_{Overall} = w_{EHD}(D_{local} + D_{semi\_glob} + D_{glob}) + w_{CLD}(D_{CLD}) \quad (17)$$

Where, w_{EHD} and w_{CLD} are the weighting coefficient of EHD and CLD methods respectively. D is the Euclidean distance. The weighting coefficients are determined by try and error algorithm for the best results.

4. EXPERIMENTAL RESULTS

4.1. Evaluation

MPEG-7 group has defined an evaluation metric called 'Average Normalized Modified Retrieval Rate (ANMRR)'

Volume: 6 Issue: 2 Pages: 2222-2232 (2014) ISSN : 0975-0290

to measure overall performance calculated by averaging the result from each query [22, 29] as:

$$ANMRR = \frac{1}{NQ}\sum_{q=1}^{NQ} NMRR(q) \quad (18)$$

where, NQ is a number of query images and NMRR stands for Normalized Modified Retrieval Rate that is used to measure the performance of each query according to:

$$NMRR(q) = \frac{\left(\sum_{k=1}^{NG(q)} \frac{Rank(k)}{NG(q)}\right) - 0.5 - \frac{NG(q)}{2}}{K(q) + 0.5 - 0.5 \times NG(q)} \quad (19)$$

where NG (q) is the size of ground truth image set for a query image q, Rank (k) is ranking of ground truth images retrieved by the retrieval algorithm and K(q) specifies a "relevance rank" for each query. A suitable K(q), because of variation of the ground truth images, is determined by:

$$K(q) = \min(4 \times NG(q), 2 \times GTM) \quad (20)$$

where GTM is the maximum of NG(q) over all queries. NMRR and ANMRR are in the range of (0, 1) and smaller values represent better retrieval performance.

4.2. Database

In order to compare the performance of studied CBIR methods based on a common database specialized for tourism application, photographs from the attractions of Zahedan city and University of Sistan and Baluchestan were taken in different times of a day and from different angles and distances. Then, the database was prepared as a two sets, image set consisting of 1000 images, and query set consisting of 21 images including a ground truth set for each query. Table 3 lists the queries and their parameters. Sample images from query set are shown in Fig. 11. A query image with its all similar images existence in database is demonstrated in Fig. 12.

	Place	NG(q)	K(q)
1	Amphitheater	34	136
2	Computer Center	25	100
3	Circular fountain	7	28
4	Stone fountain	38	152
5	Hamoon park fountain	16	64
6	Arithmetic Sculpture	16	64
7	Library	84	168
8	Jars column	9	36
9	Blue pottery	21	84
10	Statue of Ferdowsi	28	112
11	Phoenix Statue	12	48
12	Cultural buildings	17	68
13	Predecessor	20	80
14	Martyr's tomb	11	44
15	Shahriar Sculpture	11	44
16	Statue of Allameh	18	72
17	Four arch	13	52
18	Statue of Takhti	10	40
19	White Statue	15	60
20	Altar	73	168
21	Windward	26	84

Table 3: Tourism sample queries

Fig. 11: Tourism database sample images query

(a)

(b)

Fig. 12: query image #10 in the prepared database
(a) The reference image of Tourism database query #10
(b) Ground truth set of Tourism database query #10

Corel_1k database is commonly used in image retrieval researches such as SIMPLIcity [20]. It consists of 1000 images. These images are divided into 10 categories based on semantic concepts and ground truth sets of 20 sample query images from different categories. Table 4 lists the queries and their parameters.

	Query	NG(q)	K(q)
1	Beach	32	128
2	Beach	29	116
3	Rome	25	100
4	Statue	20	80
5	Blue bus	8	32

Volume: 6 Issue: 2 Pages: 2222-2232 (2014) ISSN : 0975-0290

6	Yellow bus	10	40
7	Red bus 29	29	116
8	Dino painting1	100	200
9	Dino painting2	100	200
10	Elephant 1	19	76
11	Elephant 2	20	80
12	Yellow flower	17	68
13	White flower	11	44
14	Orange flower	11	44
15	Red flower	35	140
16	Purple flower	26	104
17	Brown horse	82	200
18	White horse	47	188
19	Ice mountain	54	200
20	Mountain and grassland	26	104

Table 4: Corel_1k sample queries

Performance Comparison: Studied CBIR algorithms were applied to our database and Corel_1k to evaluate their performances. The performance evaluation was carried out in terms of ANMRR criteria and query running time. The reason for selecting the ANMRR evaluation metric is that ANMRR is defined in MPEG-7 standard to measure retrieval performance base on both, the number of correctly retrieved images and how highly these images are ranked which distinct ANMRR from other evaluation metrics such as precision and recall [22, 24, 34, 35]. Moreover, the ANMRR measure approximately coincides with the results of subjective retrieval accuracy evaluation of search engines [34]. Table 5 shows the comparison results. Furthermore, some advantages and disadvantages of the studied algorithms applied to the tourism database are listed in Table 9. According to the results, The SCD method has less computation in feature extraction and further good accuracy. The SCD algorithm provided the minimum running time (0.05 sec.) and the second best ANMRR (0.44). In the next stage, the CLD algorithm performed as the third best in terms of ANMRR and running time. Comparing to SCD method, the CLD has less ANMRR and a little more running time.

These algorithms provide the most relevant retrieved images for a query as well. This means edge and color are the most important features in this application.

Reported running time in Table 8, is only a time for extracting a query. In order to measure the running time of an algorithm in multitasking operating system environment precisely, first we measured the running time of algorithm applied to three subsets with 100, 200, and 400 images of tourism database. Then the measured running time of each subset was divided by the number of its images in order to compute the running time for an image. Finally, an average over the three running times obtained by three subsets was computed as the running time of the algorithm. The obtained running times of studied algorithms are presented in Table 8.

Results of proposed methods are also shown in Table6. Experimental results show that the semi-global and global histograms generated from the local histogram bins help to improve the retrieval performance either to tourism and corel_1k databases in comparison with local edge histogram only, because the semi-global and global edges considered the edge distribution in whole of an image.

Algorithm	Tourism ANMRR	Corel_1k ANMRR
CLD	0.4954	0.3886
DCD	0.5577	0.3691
SCD	0.4464	0.3727
Co-occurrence	0.4814	0.6105
Color feature	0.6255	0.4432
Local EHD only	0.3331	0.5603

Table 5: ANMRR results of the studied algorithms applying our tourism database and Corel_1k

Proposed Method	Tourism ANMRR	COREL_1k ANMRR
Semi-global EHD	0.4088	0.6169
global EHD	0.3641	0.6116
EHD(Local+semiglobal+global)	0.3021	0.5579

Table 6: ANMRR results of the proposed algorithms applying our tourism database and Corel_1k

Next, we apply HSV color space instead of YCbCr and RGB color spaces in CLD and color feature algorithms. Therefore, we achieve higher retrieved results applying HSV color space in our prepared tourism database; which means HSV color space is more suitable for our prepared tourism database. Results of this experiment are shown in Table 7.

Algorithm	By HSV_ANMRR	Without HSV_ANMRR
Color	0.535	0.4432
CLD	0.467	0.3691

Table 7: ANMRR results of applying HSV color space in some algorithms for Tourism database

Finally, EHD and CLD are combined applying Equation (17) using following weighting coefficients.

$w_{CLD} = 0.348$

$w_{EHD} = 0.652$

Concluded ANMRR by combining these two methods is obtained 0.275 which is the best and the smallest ANMRR resulted for the tourism database.

Fig. 13 and Fig. 14 respectively demonstrate retrieval results of two sample query images: #10 "Statue of Ferdowsi" in Tourism database and #7 "red bus" in Corel_1k applying some of the studied methods. In these two figures, the left-upper image marked by a solid black line is a query (1^{st} ranked image) and the other images are displayed in a raster scan order according to their retrieval ranks.

Volume: 6 Issue: 2 Pages: 2222-2232 (2014) ISSN : 0975-0290

Method	CLD	EHD	Co-occurrences	SCD	DCD
Time(sec)	0.0510	0.6206	0.1402	0.050	4.0221

Table 8: Query running Time results of the studied algorithms applying our tourism database

Method	Advantages	Disadvantages
CLD	- Considering local color information - Less sensitivity to fast color variation - Low running time - Good accuracy	- Not considering edge information
EHD	- Considering local edge information - Best accuracy	- Not considering color information - High running time
Co-occurrences	- Considering texture information	- Not considering color & edge information
SCD	- Low running time - Considering color information - Good accuracy	- Not considering edge information - No local information
DCD	- Considering color information	- Not considering edge information - No local information - High running time - Low retrieval performance

Table 9: Advantages and disadvantages of the studied algorithms applying our tourism database

5. CONCLUSIONS

In this paper a scenario for using of CBIR in tourism application was proposed. Several CBIR algorithms were studied. An image database specialized for the proposed scenario was prepared. All the studied algorithms were applied to both of the databases; our prepared tourism and Corel_1k. Performance evaluation of all the algorithms was compared based on the ANMRR criteria.

(a)

(b)

Volume: 6 Issue: 2 Pages: 2222-2232 (2014) ISSN : 0975-0290

(c)

Fig. 13: Retrieval results of our prepared Tourism database
(a) Retrieval results of MPEG-7 CLD (NMRR=0.3070). 12 of 28 ground truth images found in the first 20 retrievals.
(b) Retrieval results of MPEG-7 EHD (NMRR=0.1523). 14 of 28 ground truth images found in the first 20 retrievals.
(c) Retrieval results of proposed combining EHD and CLD (NMRR=0.1523). 15 of 28 ground truth images found in the first 20 retrievals

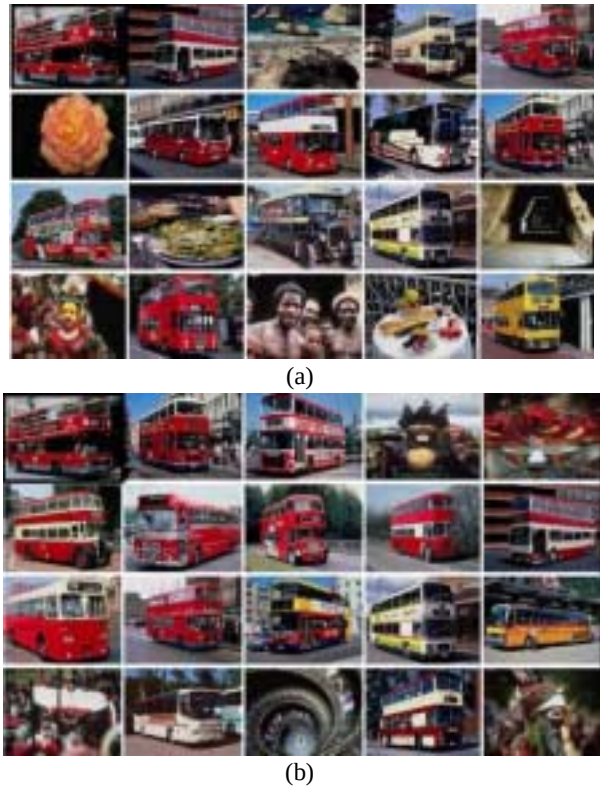

(a)

(b)

Fig. 14: Retrieval results for Corel_1k database

(a) Retrieval results of SCD (NMRR=0.5005). 7 of 29 ground truth images found in the first 20 retrievals.
(b) Retrieval results for Corel_1k database of DCD (NMRR=0.4106). 10 of 29 ground truth images found in the first 20 retrievals.

After comparison, among all the studided algorithms, EHD, SCD and CLD algorithms were selected as the best retrieval algorithms for prepared tourism database even DCD algorithm had the best retrieval results in Corel_1k database. Finally by modification of combining CLD and EHD, a new CBIR algorithm is proposed for tourism application. Results of experimental work in tourism database applying new algorithm showed a high retrieval performance with ANMRR=0.2751. In addition, it is found that HSV color space is the best color space for our prepared tourism database especially in applying color features CBIR algorithms. Furthermre, among all the algorithms, SCD had the most less running time in both of the databases.

REFERENCES

[1]. S.Y. An, L.K. Lee, S.Y. Oh, ‘Modified angular radial partitioning for edge image description in image retrieval’, Electronics Letters, Vol. 48, pp. 563-565, 2012

[2]. C.Young Deok, K. Nam Chul, J. Ick Hoon, ‘Content-Based Image Retrieval Using Multiresolution Color and Texture Features’, IEEE Transactions on Multimedia, Vol. 10, pp. 1073-1084, 2008

[3]. C. Chin-Chen, W. Wen-Chuan, H. Yu-Chen, ‘Content-Based Color Image Retrieval System Using Color Difference Features’, Future Generation Communication and Networking Symposia, pp. 181-184, 2008

[4]. L. Fei, D. Qionghai, X. Wenli, G.Er, ‘Multilabel Neighborhood Propagation for Region-Based Image Retrieval’, IEEE Transactions on Multimedia,Vol. 10, pp. 1592-1604, 2008

[5]. M.J. Swain, D.H. Ballard, ‘Color indexing’, Int. J. Computer Vision, Vol. 7, no. (1), pp. 11-32, 1991

[6]. H. Tamura, S. Mori, T. Yamawaki, ‘Textural Features Corresponding to Visual Perception’, IEEE Transactions on Systems, Man and Cybernetics, Vol. 8, pp. 460-473, 1978

[7]. Y. Liu, D. Zhang, G. Lu, W.-Y. Ma, ‘A survey of content-based image retrieval with high-level semantics’, Pattern Recognition, Vol. 40, (1), pp. 262-282, 2007

[8]. X.-Y. Wang, Y.-J. Yu, H.-Y. Yang, ‘An effective image retrieval scheme using color, texture and shape features’, Computer Standards & Interfaces, Vol. 33, pp. 59-68, 2011

[9]. X. Bai, W. Liu, ‘Research of Image Retrieval Based on Color’, Computer Science-Technology and Applications. IFCSTA '09, pp. 283-286, 2009

Volume: 6 Issue: 2 Pages: 2222-2232 (2014) ISSN : 0975-0290

[10]. Y. Rui, T.S. Huang, S.F. Chang, 'Image Retrieval: Current Techniques, Promising Directions, and Open Issues', Journal of Visual Communication and Image Representation, Vol. 10, pp. 39-62, 1999

[11]. G.-H. Liu, J.-Y Yang, 'Image retrieval based on the texton co-occurrence matrix', Pattern Recognition, Vol. 41, pp. 3521-3527, 2008

[12]. G.R. Cross, A.K. Jain, 'Markov Random Field Texture Models', IEEE Transactions on Pattern Analysis and Machine Intelligence , Vol. PAMI-5, pp. 25-39, 1983

[13]. J. Mao, A.K. Jain, 'Texture classification and segmentation using multiresolution simultaneous autoregressive models', Pattern Recognition, Vol. 25, pp. 173-188, 1992

[14]. F. Liu, R.W. Picard, 'Periodicity, directionality, and randomness: Wold features for image modeling and retrieval', IEEE Transactions on Pattern Analysis and Machine Intelligence, Vol. 18, pp. 722-733, 1996

[15]. B.S. Manjunath, W.Y. Ma, 'Texture features for browsing and retrieval of image data', IEEE Transactions on Pattern Analysis and Machine Intelligence, Vol. 18, pp. 837-842, 1996

[16]. E.Yildizer, A.M. Balci, T.N. Jarada, R. Alhajj, 'Integrating wavelets with clustering and indexing for effective content-based image retrieval', Knowledge-Based Systems, Vol. 31, pp. 55-66, 2012

[17]. A. Amanatiadis, V.G. Kaburlasos, A.Gasteratos, S.E. Papadakis, 'Evaluation of shape descriptors for shape-based image retrieval', IET Image Processing, Vol. 5, pp. 493-499, 2011

[18]. Z. Raisi, F. Mohanna, M. Rezaei, " Content-Based Image Retrieval for Tourism Application Using Handheld Devices", IJICTR Journal, Vol. 4, pp. 57-64, 2011

[19]. I. Ahmad, M. Gabbouj, 'A generic content-based image retrieval framework for mobile devices', Multimed Tools Appl, Vol. 55, pp. 423-442, 2011

[20]. J.Z. Wang, L. Jia, G. Wiederhold, 'SIMPLIcity: semantics-sensitive integrated matching for picture libraries', IEEE Transactions on Pattern Analysis and Machine Intelligence, Vol. 23, pp. 947-963,2001

[21]. S.J.P. Sung Min Kim, Chee Sun Won, 'Image Retrieval via Query-by-Layout Using MPEG-7 Visual Descriptors', ETRI Journal, Vol. 29, pp. 246-248, 2007

[22]. B.S. Manjunath, J.R. Ohm, V.V. Vasudevan, A. Yamada, 'Color and texture descriptors', IEEE Transactions on Circuits and Systems for Video Technology, Vol. 11, pp. 703-715, 2011

[23]. D.K. Park, Y.S. Jeon, C.S. Won, 'Efficient use of local edge histogram descriptor'. Proc. Proceedings of the 2000 ACM workshops on Multimedia, Los Angeles, California, United States, 2000

[24]. R. Balasubramani, D.V.K., 'Efficient use of MPEG-7 Color Layout and Edge Histogram Descriptors in CBIR Systems', Global Journal of Computer Science and Technology, pp. 157-163, 2009

[25]. F.Z. Hesamoddin Salehian, 'Fast Content Based Color Image Retrieval System Based on Texture Analysis of Edge Map', Advanced Materials Research, Vol. 341-342, pp. 168-172, 2011

[26]. S. Hong, W. Yueshu, C. Wencheng, Z. Jinxia, 'Image Retrieval Based on MPEG-7 Dominant Color Descriptor', The 9th International Conference for Computer Scientists, 18-21 Nov. 2008.

[27]. N.-C.Yang, W.-H. Chang, C.-M. Kuo, T.-H. Li, 'A fast MPEG-7 dominant color extraction with new similarity measure for image retrieval', J. Vis. Common. Image Represent. Vol. 19, pp. 92-105, 2008

[28]. A. Ibrahim, A.a.A. Zou'bi, R. Sahawneh, M. Makhadmeh, 'Fixed Representative Colors Feature Extraction Algorithm for Moving Picture Experts Group-7 Dominant Color Descriptor', Journal of Computer Science, Vol. 5, pp. 773-777

[29]. A. Ibrahim, R. Sahawneh, M. Makhadmeh, 'Fixed Representative Colors Feature Extraction Algorithm for Moving Picture Experts Group-7 Dominant Color Descriptor ', Journal of Computer Science, Vol. 5, pp. 773-777, 2009

[30]. N.C. Yang, W.H Chang, C.M. Kuo, T.H. Li, A fast MPEG-7 dominant color extraction with new similarity measure for image retrieval. Journal of Visual Communication and Image Representation, Vol. 19, pp. 92-105, 2008

[31]. K. Konstantinidis, A. Gasteratos, I. Andreadis, 'Image retrieval based on fuzzy color histogram processing', Optics Communications, Vol. 248, pp. 375-386, 2005

[32]. S.-Y.C. Cheng-Hao Yao,'Retrieval of translated, rotated and scaled color textures', Pattern Recognition ,Vol. 36, pp. 913-929, 2003

[33]. E. Yildizer, A.M.B., T. N. Jarada, R. Alhajj, 'Integrating wavelets with clustering and indexing for effective content-based image retrieval', Knowledge-Based Systems, 2012

[34]. P. Ndjiki-Nya, J.R., T. Meiers, J.-R. Ohm, A. Seyferth, R. Sniehotta, 'Subjective Evaluation of the MPEG-7 Retrieval Accuracy Measure (ANMRR)', 2000

[35]. K.M. Wong, 'Content Based Image Retrieval Using MPEG-7 Dominant Descriptor', University of Hong Kong, 2004